



Supplement of

Black carbon content of traffic emissions significantly impacts black carbon mass size distributions and mixing states

Fei Li et al.

Correspondence to: Ye Kuang (kuangye@jnu.edu.cn) and Jun Zhao (zhaojun23@mail.sysu.edu.cn)

The copyright of individual parts of the supplement might differ from the article licence.

27 **S1. Particle number size distributions inverted from DMA-SP2 measurements and multiple**
28 **charging corrections**

29 The aerosol number concentrations at mobility diameter D_p measured by the SP2 represent the
30 number concentration of aerosols in a diameter range with half width of the electrical mobility as
31 $\Delta Z_p = Z_p \frac{Q_a}{Q_{sh}}$, where Z_p is the electrical mobility corresponding to D_p , Q_a is the SP2 sample flow
32 (0.1 L/min) and Q_{sh} is the DMA sheath flow (2 L/min). Therefore, if we term the measured aerosol
33 number concentration as $\Delta N(D_p)$, the corresponding $\Delta \log(D_p)$ can be calculated based on ΔZ_p ,
34 with the relationship between Z_p and D_p as $Z_p = \frac{neC(D_p)}{3\pi\mu D_p}$, where e is the elementary charge, μ is the
35 gas viscosity coefficient, and $C(D_p)$ is the Cunningham slip correction factor.

36 The size distributions with only transmission efficiency of single charge particles accounted for
37 can be formulated as:

38
$$\frac{dN(D_p)}{d\log(D_p)} = \frac{\Delta N(D_p)}{\Delta \log(D_p)} / R,$$

39 where R is the known transfer efficiency ratio of mobility diameter. Then, multiple charging
40 correction of one-dimensional size distribution can be conducted as described in Zhao et al. (2021a).

41 One the basis of this, the particle number size distributions (PNSD) of BC-free aerosols and BC-
42 containing aerosols are also be derived. Following Zhao et al. (2021a), multiple charging corrections
43 were conducted separately for BC-containing and BC-free aerosols. The distribution of BC-
44 containing aerosols could be described using a two-variable function $\frac{\partial N}{\partial \log(D_p) \partial \log(D_c)}$, where D_c is
45 the BC core diameter. The D_c was divided into 30 different bins from 80 to 500 nm, where the $\Delta \log$
46 D_c was the same for different bins. For each D_c bin, there was only D_p dimension for the size
47 distribution, therefore, the multiple charging correction can be applied.

48 **S2. PMF analysis**

49 An improved source apportionment technique called Multilinear Engine (ME-2) were used to
50 deconvolve organic aerosol (OA) spectra measured by the Q-ACSM into OA factors. Different from
51 traditional PMF, ME-2 offers a coefficient called a-value to constrain the spectral variation extent of
52 OA factor with given priori mass spectra. The unconstrained runs with PMF technique were firstly
53 performed with a possible factor number of 2-8, and diagnostics analysis were shown in Fig.S1, and
54 the three factors solution seems the best solution, and the spectral and time series analysis of factors

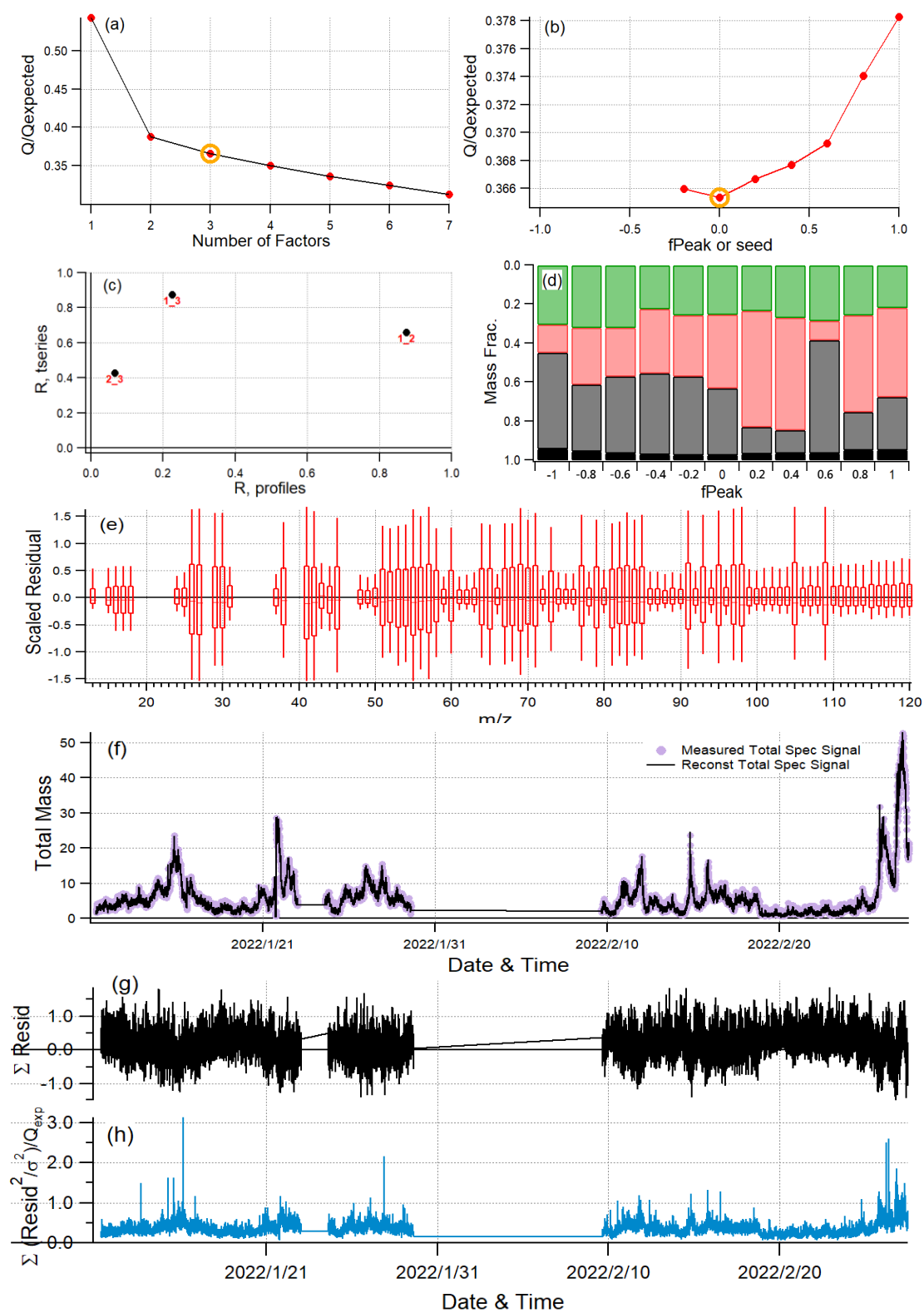
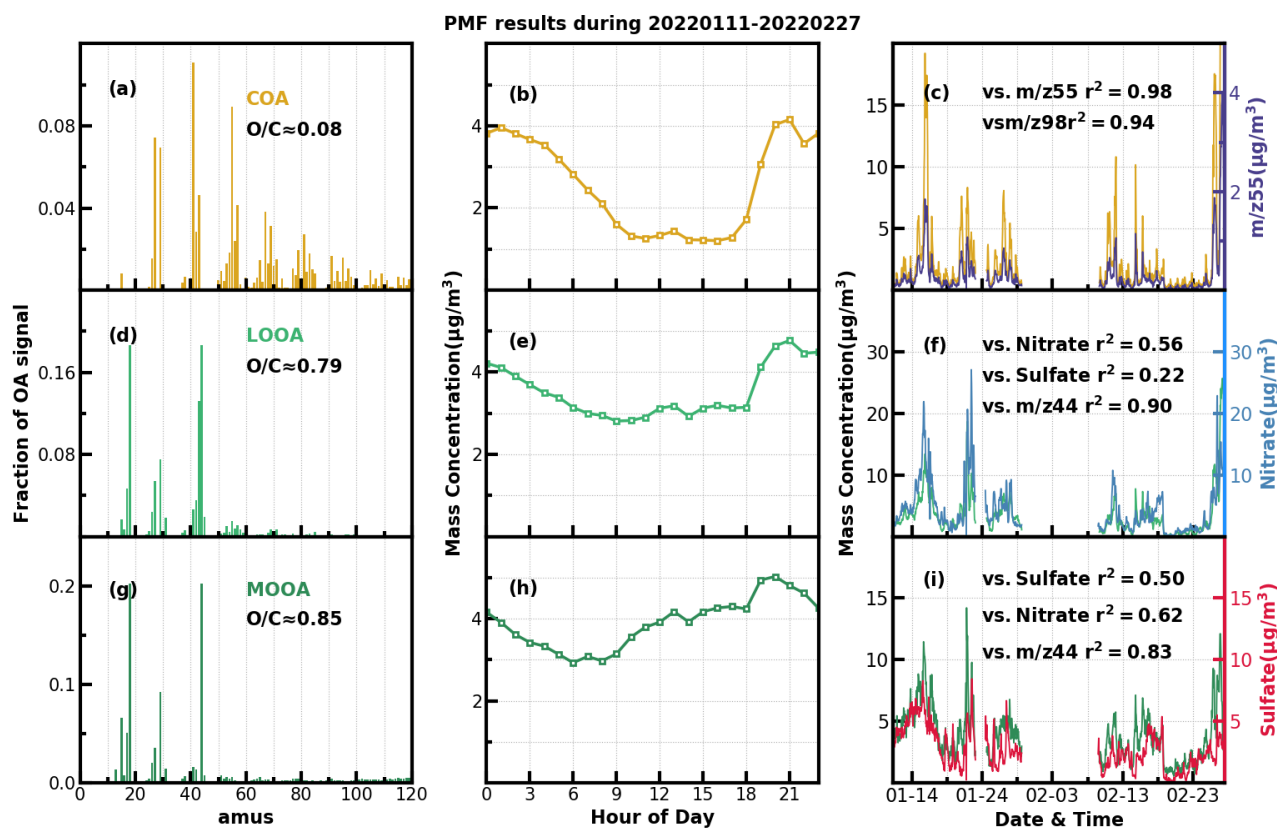


Figure S1. Diagnostic plots of the 3-factor solution in the unconstrained PMF.

55 are shown in Fig. S2. It shows clearly a primary organic aerosol factor (POA), s less-oxidized
 56 oxygenated organic aerosol factor (OOA) and a more-oxidized oxygenated organic aerosol factor
 57 (MOOA). However, three factors solution does not split two major primary OA factors of cooking-

58 like OA (COA) and hydrocarbon-like OA (HOA) in urban area. Therefore, we had chosen 4 factors
 59 for ME-2 analysis and constrained the COA profile with the a value ranging from 0.1 to 0.5. The



60 Figure S2. The spectral characteristics, diurnal variations and time series analysis of three factors resolved by the PMF
 61 COA profile reported in Liu et al. (2022) as a proxy was used considering the following three
 62 reasons: (1) The used instrument of this study is the same one of Liu et al. (2022); (2) the COA
 63 profile reported in Liu et al. (2022) was determined during the period when both COVID-19 silence-
 64 action and festival spring occurred when cooking activities grew and traffic activities almost
 65 vanished thus COA shall dominated over HOA. More details regarding the method can be referred to
 66 Liu et al. (2022); (3) Resolved variations of HOA and COA are well explained by external datasets
 67 such as correlations of HOA with black carbon whose correlation coefficient could reach 0.88. The
 68 four-factor solution using the ME-2 technique with $a=0.1$ was obtained and was shown in Fig. S3.

68
 69
 70
 71

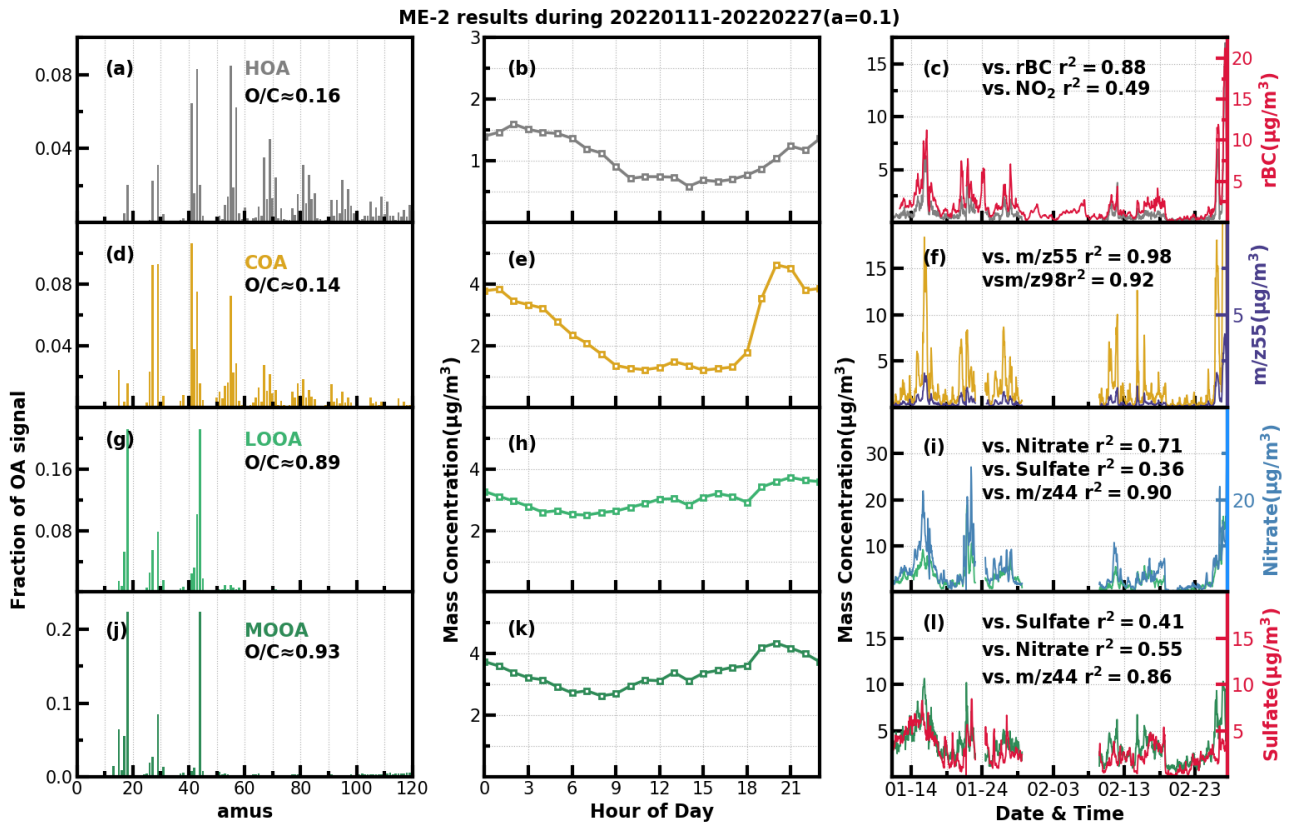


Figure S3. Mass spectral profiles, diurnal cycles and correlations with external data of COA(a-c), HOA(d-f), LOOA(g-i) and MOOA(j-l) from ME2-ACSM analysis.

72 **S3. BC measurements from AE33**

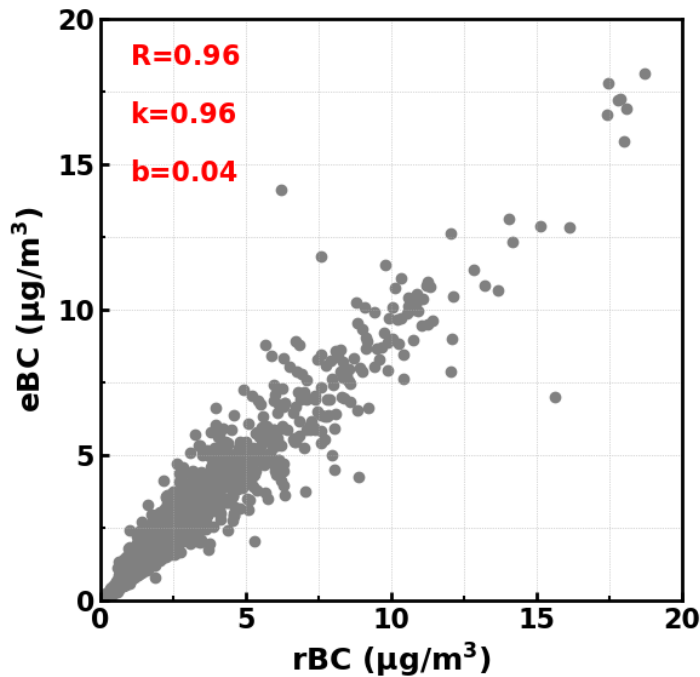


Figure S4. Comparison between rBC derived from DMA-SP2 measurements and optical equivalent BC (eBC) derived from AE33 measurements.

73 The AE33 measurements are on the basis of filter collection which would lead absorption
74 measurements be biased due to loading effect and multiple scattering effect. AE33 used dual-spot mode
75 for dealing with aethalometer loading effect (Drinovec et al., 2015). However, a Multiple-scattering
76 correction factor (C) was still needed to convert measured attenuation coefficient to the absorption
77 coefficient of ambient aerosols. Results of previous studies demonstrate that C is mainly associated
78 with filter tape, however, might also varies with aerosol chemical compositions (Wu et al.,
79 2009;Collaud Coen et al., 2010), the filter tape 8060 was used for AE33 in this study. Zhao et al. (2020)
80 estimated C of filter tape 8060, and their results demonstrated that C is almost independent of
81 wavelength and differs little among measurements of different locations, and reported an average C
82 value of 2.9 with the default C of AE33 is 1.57 (Drinovec et al., 2015). On the other hand, the
83 derivations of optically equivalent BC (eBC) mass concentrations from AE33 measurements needs a
84 priori mass absorption cross section (MAC) which actually varies much in the atmosphere (Zhao et al.,
85 2021b). In our previous measurements in the North China Plain (not published), we found that if
86 default C and default MAC (7.77 m²/g at 880 nm) were used, the derived eBC concentrations agree
87 generally well with DMA-SP2 measurements which further demonstrated as shown in Fig.S4.
88 Therefore, the default C and MAC was directly used for eBC concentration derivations in this study.

89

90 **Fitting form of BCMSD:**

$$91 \frac{dM_{BC}}{d\log D_p} = \frac{M_{BC}}{\sqrt{2\pi} \log(\sigma_g)} \cdot \exp\left(-\frac{[\log(D_p) - \log(D_{g,BC})]^2}{2 \log(\sigma_g)^2}\right) \quad (S1)$$

92

93 **References**

94 Collaud Coen, M., Weingartner, E., Apituley, A., Ceburnis, D., Fierz-Schmidhauser, R., Flentje, H., Henzing, J. S., Jennings,
95 S. G., Moerman, M., Petzold, A., Schmid, O., and Baltensperger, U.: Minimizing light absorption measurement artifacts of
96 the Aethalometer: evaluation of five correction algorithms, *Atmos. Meas. Tech.*, 3, 457-474, 10.5194/amt-3-457-2010,
97 2010.

98 Drinovec, L., Močnik, G., Zotter, P., Prévôt, A. S. H., Ruckstuhl, C., Coz, E., Rupakheti, M., Sciare, J., Müller, T., Wiedensohler,
99 A., and Hansen, A. D. A.: The "dual-spot" Aethalometer: an improved measurement of aerosol black carbon with real-
100 time loading compensation, *Atmospheric Measurement Techniques*, 8, 1965-1979, 10.5194/amt-8-1965-2015, 2015.

101 Liu, L., Kuang, Y., Zhai, M., Xue, B., He, Y., Tao, J., Luo, B., Xu, W., Tao, J., Yin, C., Li, F., Xu, H., Deng, T., Deng, X., Tan, H., and
102 Shao, M.: Strong light scattering of highly oxygenated organic aerosols impacts significantly on visibility degradation,
103 *Atmos. Chem. Phys.*, 22, 7713-7726, 10.5194/acp-22-7713-2022, 2022.

104 Wu, D., Mao, J., Deng, X., Tie, X., Zhang, Y., Zeng, L., Li, F., Tan, H., Bi, X., Huang, X., Chen, J., and Deng, T.: Black carbon
105 aerosols and their radiative properties in the Pearl River Delta region, *Science in China Series D: Earth Sciences*, 52, 1152-
106 1163, 10.1007/s11430-009-0115-y, 2009.

107 Zhao, G., Yu, Y., Tian, P., Li, J., Guo, S., and Zhao, C.: Evaluation and Correction of the Ambient Particle Spectral Light
108 Absorption Measured Using a Filter-based Aethalometer, *Aerosol and Air Quality Research*, 20, 1833-1841,
109 10.4209/aaqr.2019.10.0500, 2020.

110 Zhao, G., Tan, T., Zhu, Y., Hu, M., and Zhao, C.: Method to quantify black carbon aerosol light absorption enhancement
111 with a mixing state index, *Atmos. Chem. Phys.*, 21, 18055-18063, 10.5194/acp-21-18055-2021, 2021a.

112 Zhao, W., Tan, W., Zhao, G., Shen, C., Yu, Y., and Zhao, C.: Determination of equivalent black carbon mass concentration
113 from aerosol light absorption using variable mass absorption cross section, *Atmos. Meas. Tech.*, 14, 1319-1331,
114 10.5194/amt-14-1319-2021, 2021b.

115